

Focusing-Schlieren PIV Measurements of a Supersonic Turbulent Boundary Layer

Michael J. Hargather*, Michael J. Lawson†, Gary S. Settles‡

Penn State Gas Dynamics Laboratory, University Park, Pennsylvania, 16802, USA

Leonard M. Weinstein§

National Institute of Aerospace, Hampton, Virginia, 23666, USA

Sivaram Gogineni¶

Spectral Energies, LLC, Dayton, Ohio, 45434, USA

A focusing-schlieren optical system has been developed for performing velocity measurements in refractive turbulent flows using commercial particle image velocimetry (PIV) algorithms. Focusing-schlieren optics allows the visualization of refractive disturbances within a limited depth-of-focus, resulting in quasi-planar schlieren images. The schlieren “PIV” technique makes use of naturally-occurring refractive-turbulent eddies in a flow as PIV “particles” upon which velocimetry is performed. Current experiments are performed in a small supersonic wind tunnel to measure the Mach 3 turbulent boundary layer mean-velocity profile. Results from both focusing-schlieren PIV and shadowgraph PIV are compared to the velocity profile from a standard pitot-pressure survey. The natural intermittency of the outer part of the turbulent boundary layer plays a role in the schlieren PIV results, but useful measurements of the velocity profile can still be made. We also introduce an important improvement in schlieren “PIV”, the use of a pulsed LED light source in place of the twin pulsed lasers typically required for traditional PIV measurements. This comparatively-inexpensive white-light source eliminates the traditional problems of laser illumination in schlieren optical systems and improves the overall results.

Nomenclature

| | |
|------------|--|
| PIV | Particle Image Velocimetry |
| DOF | Depth-of-focus |
| LED | Light Emitting Diode |
| l | length from schlieren lens to plane-of-focus |
| l' | length from schlieren lens to image plane |
| L | length from schlieren lens to source grid |
| L' | length from schlieren lens to cutoff grid |
| A | length of aperture |
| a | schlieren cutoff length fraction |
| ϵ | schlieren sensitivity |
| γ | intermittency function |
| ζ | intermittency function parameter |

*Senior Research Associate, Department of Mechanical and Nuclear Engineering, 208 Reber Building, University Park, PA, 16802, AIAA Member

†Graduate Research Assistant, Department of Mechanical and Nuclear Engineering, 301D Reber Building, University Park, PA, 16802, AIAA Member

‡Distinguished Professor of Mechanical Engineering and Director of Penn State Gas Dynamics Laboratory, Department of Mechanical and Nuclear Engineering, 301D Reber Building, University Park, PA, 16802, AIAA Associate Fellow

§Senior Research Fellow, National Institute of Aerospace, 100 Exploration Way, Hampton VA, 23666, AIAA Associate Fellow

¶President, Spectral Energies, LLC, 2238 Hunters Ridge Blvd, Dayton, OH, 45434, AIAA Fellow

| | |
|------------|--|
| σ | standard deviation |
| δ | boundary layer height |
| y | distance perpendicular to tunnel floor |
| u | local flow velocity |
| U_∞ | freestream velocity |

I. Introduction

Particle image velocimetry (PIV) is a well-known and widely-used technique for measuring planar velocity distributions in a range of fluid-dynamic systems. Typically, particles suspended in the moving fluid are tracked using a series of digital image pairs to determine local flow velocities.¹ Situations arise, however, where the use of tracer particles is impractical or impossible, thus traditional PIV cannot be used. This has given rise to current interest in “seedless velocimetry”, in which something other than solid particles is tracked. One experimental method that can be used in some of these situations is schlieren “PIV”.

Schlieren “PIV” is the technique of combining PIV equipment and software with schlieren optics for the purpose of seedless velocimetry measurements in refractive turbulent flows.² Turbulent flows are naturally “seeded” by eddies of various scales that travel at the local convective speed of the flow. Velocimetry can thus be performed, without the need for particulate seeding, by correlating eddy motion between two consecutive schlieren or shadowgraph images. However, this approach relies upon both turbulence and refractive-index gradients in the flow, thus limiting its range of applicability. Nonetheless it naturally lends itself to high-Reynolds number compressible flows, where both these conditions are met. Low-speed turbulent flows can also be measured this way if a refractive thermal or species difference is imposed.

Schlieren velocimetry was first proposed by Townend,³ but it proved impractical in the pre-computer age. Papamoschou^{4,5} revisited the technique, using a pattern-matching algorithm to track eddy motion in supersonic shear layers. Fu and Wu⁶ used schlieren images and image-analysis software to measure velocity distributions in gas fires and explosions. The schlieren “PIV” technique was substantially improved by Jonassen et al.² by the use of a commercially-available PIV system to measure velocity profiles in a helium jet in air and a supersonic turbulent boundary layer.

One observed disadvantage in prior schlieren “PIV” studies is the integrating property of traditional schlieren optics along the optical path.⁷ The eddy motion recorded in the two consecutive “PIV” images includes all motion across the entire flowfield, thus yielding a path-averaged measurement of the convective eddy speed. Thus, near-planar velocimetry is not possible using traditional schlieren optics, as it is in traditional particle PIV with laser-sheet illumination. This limits the utility of schlieren “PIV” in three-dimensional flows.

In order to perform near-planar measurements, “focusing schlieren” optics are required. The lens-and-grid schlieren method, originally proposed by Schardin⁸ in order to achieve a large field-of-view inexpensively, naturally also has a limited depth-of-focus for refractive disturbances. This technique, recently perfected by Weinstein,⁹ images refractive disturbances within a limited depth-of-focus while disturbances outside this region are too blurred to register in the image.⁷ Alvi et al.¹⁰ combined this focusing schlieren approach with an optical deflectometer to perform pointwise measurements of turbulence within a low-speed axisymmetric jet. Garg and Settles¹¹ extended this point-wise approach to measurements of a supersonic turbulent boundary layer.

The present work develops a focusing-schlieren “PIV” instrument and tests it by measuring the velocity profile in a two-dimensional turbulent boundary layer at Mach 3 in the Penn State Gas Dynamics Laboratory’s supersonic wind tunnel. The thick wind-tunnel-tunnel floor boundary layer provides a well-characterized flow which is used as a benchmark for present purposes. Turbulent eddy motion is captured by a PIV camera and quantified with PIV software, whereby boundary-layer velocity data are extracted.

II. Experimental Methods

The experimental methods required for this effort include the focusing schlieren optical system, a pulsed LED light source that provides the necessary PIV-type illumination, the supersonic wind tunnel facility, and the commercial PIV hardware/software used here. For comparison, conventional non-focusing shadowgraphy is also used.

II.A. Focusing Schlieren Optical System

Using the approach proposed by Weinstein,⁹ a focusing-schlieren system was designed to image the present Mach 3 compressible turbulent boundary layer, and for related purposes. The basics of the lens-and-grid schlieren method used here are described by Settles.⁷ A schematic of the focusing optical system is given in Figure 1. The optical components include a Fresnel lens and an 80mm-aperture $f/3.8$ imaging lens, along with complementary source and cutoff grids. The source grid is an array of horizontal clear-and-opaque bands that function as multiple schlieren light sources at various angles with the optical centerline. The cutoff grid is a photographic negative of the source grid and is located in a plane optically conjugate to it. By adjusting the cutoff grid to block a fraction of the light from reaching the image plane, the schlieren effect is achieved.

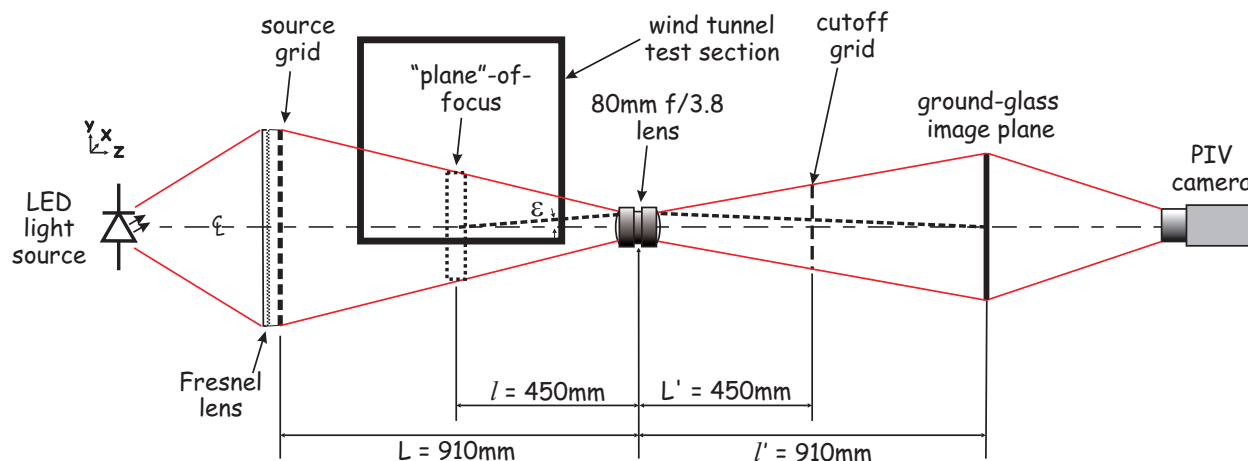


Figure 1. Schematic of the focusing schlieren optical system

Due to the convergence of the schlieren light-beam between the source grid and the imaging lens, the narrow “plane”-of-focus is reconstructed in the vicinity of an optically-conjugate plane, designated the “image plane” as illustrated in Figure 1. The limited depth-of-focus inside the wind-tunnel test section is defined by Weinstein⁹ as the depth at which a predetermined-length-scale structure is effectively blurred due to being out of focus. The so-called “un-sharp DOF” is proportional to the distance l and inversely proportional to the aperture of the schlieren lens, A :

$$\text{DOF} \propto \frac{l}{A} \quad (1)$$

The sensitivity, ϵ , of a lens-and-grid schlieren system is defined by Settles⁷ as:

$$\epsilon \propto \frac{aL}{L'(L-l)} \quad (2)$$

where a is a measure of the schlieren cutoff and ϵ is the minimum detectable refraction angle within the “plane”-of-focus. Equations 1 and 2 demonstrate that the depth-of-focus and the schlieren sensitivity are coupled. In general, schlieren sensitivity is a direct function of the strength of refractive-index gradients within the depth-of-focus, but an inverse function of the depth-of-focus itself. For a given refractive disturbance, as the depth-of-focus narrows, the schlieren sensitivity decreases toward zero. Thus a focusing-schlieren system must maintain a finite depth-of-focus and cannot be focused upon a true plane.

Given this tradeoff, higher schlieren sensitivity is sometimes preferable to a narrower depth-of-focus. One way to improve the schlieren sensitivity as well as the image illumination is to remove the image plane in Figure 1 and project the light beam directly into the PIV-camera lens. This approach, however, increases the system depth-of-focus by reducing its effective aperture, A , due to the small aperture of the camera lens.

To avoid this issue but still maintain high image illumination, one can remove the PIV-camera lens and position the camera sensor at the image plane location in Figure 1. This technique forms the focused-schlieren image directly on the camera sensor, thus retaining the same depth-of-focus as with a ground glass screen in the image plane. However, this requires a camera sensor significantly larger than those found in most or all available PIV cameras.

A ground-glass screen in the image plane of Figure 1 leads to a significant loss of schlieren illumination due to light scattering. This problem can be addressed in part by replacing the ground glass with a holographic screen that scatters less light, or by imaging directly onto the camera sensor as stated above. Unfortunately the present optical system does not have sufficient illumination or camera sensor size to allow either of these solutions. Instead, the image-plane ground-glass was removed and the schlieren beam was projected directly into the camera lens by way of a large simple lens in the image-plane position. We have thus accepted the concomitant loss of depth-of-focus in favor of image illumination for the present experiments. Future investigations with a larger LED array are expected to improve illumination enough to permit a real image on a screen in the image plane, thus a better depth-of-focus.

The depth-of-focus of the present system was experimentally determined using a 1mm-diameter over-expanded-supersonic air jet. In the plane-of-best-focus, the shock diamonds in this jet are clearly seen as shown in Figure 2. The jet was then traversed in 1mm increments away from the plane-of-best-focus until the shock diamonds were no longer distinguishable from the background, thus defining the un-sharp DOF. Figure 2 shows that the present system has a depth of focus of about $\pm 10\text{mm}$ when a screen is present in the image plane. However, the depth-of-focus increased to about $\pm 40\text{mm}$ with the image plane removed, which was the case for all present velocimetry experiments.

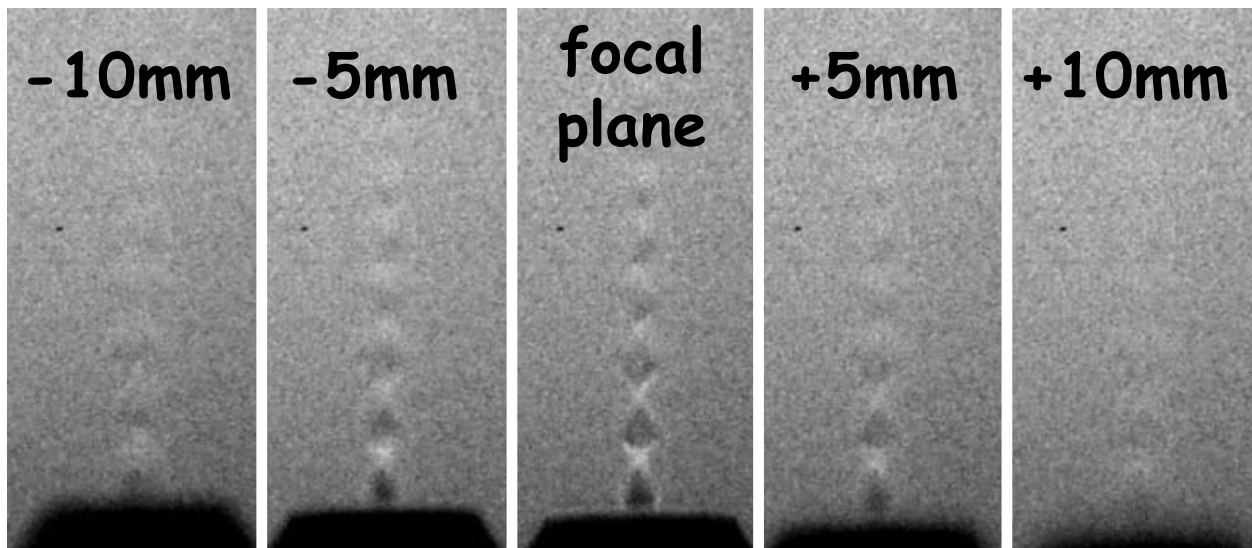


Figure 2. Demonstration of the depth-of-focus for the focusing schlieren system with a ground-glass image plane, as shown in Figure 1

II.B. LED light source

Early experiments with this optical system used a dual-head Nd:YAG laser as the light source, but significant problems with coherent artifact noise and other laser-related problems led us to explore the development of an alternative white-light source. (Laser illumination is important to produce a light-sheet in traditional PIV, but not here.)

In order to be effective for velocimetry of high speed flows, the schlieren “PIV” light source must produce two bright illumination pulses with pulse widths and interval between pulses in the microsecond range. Prior work² showed that xenon flashlamps cannot readily meet this requirement because their illumination decreases too slowly after the peak is reached. Light-emitting-diodes (LEDs), on the other hand, have been shown to pulse in the microsecond range with the desired square-wave illumination profile.¹² The key question is whether an LED source can produce enough illumination for focusing schlieren “PIV”.

An LED light source was developed for present purposes using four 15W high-power cool-white LEDs obtained from Mouser Electronics, Inc. These LEDs were found to be capable of producing a $0.5\mu\text{s}$ illumination pulse, with rise and fall times of less than $0.05\mu\text{s}$. The present 2x2 LED array, shown in Figure 3, was double-pulsed with an inter-pulse interval ranging from 1 to $2\mu\text{s}$. The Figure reveals that each LED dome contains four separate emitters.

Figure 4 presents the circuit diagram for the LED-array pulse driver. For PIV illumination, the LED

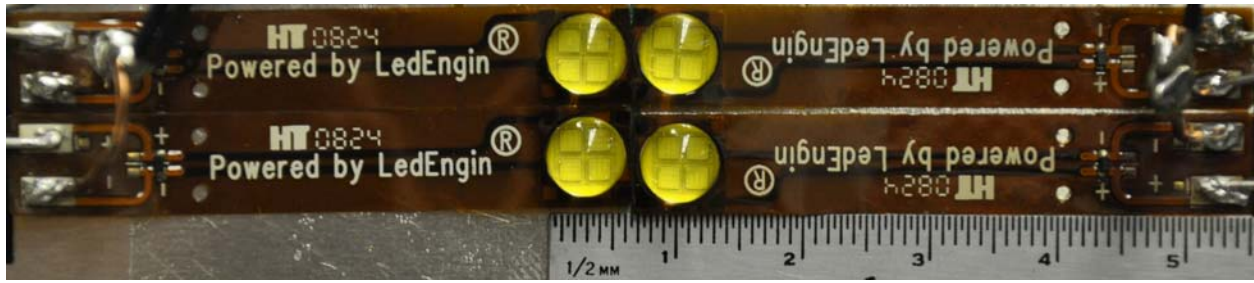


Figure 3. Image of the 2x2 LED array with a scale in millimeters

drive input is a pair of microsecond-range 15V square waves with variable pulse widths and pulse separation. This is achieved using the hex-inverter Schmitt-trigger integrated circuit modules shown. for a broader discussion of microsecond LED pulsing circuits, see O'Hagan et al.¹²

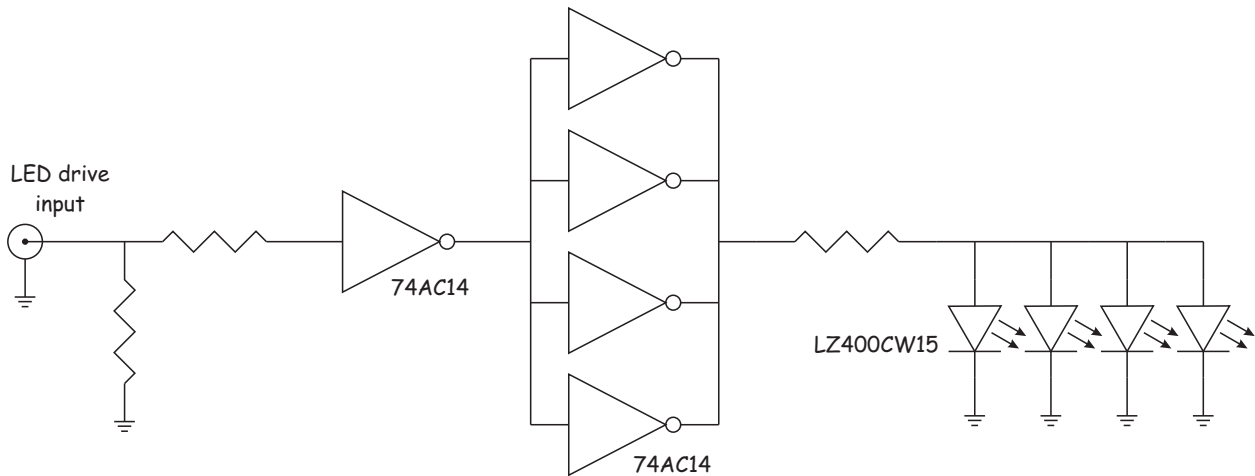


Figure 4. Circuit diagram for the 2x2 LED array

This light source showcases some of the advantages of modern LEDs as schlieren light sources: high output of non-coherent white light, quick response time, small physical size, long lifetime, and low cost. White-light illumination of the present schlieren system yielded images that could be readily processed via background subtraction and histogram modification to reveal turbulent eddies. This is typically much more difficult with traditional PIV-laser illumination from separate laser heads; heavy speckle competes with the eddies during image processing and analysis.

The quick response time of present LEDs allows their use for PIV, where brief light pulses are especially required for high-speed flows. The LED setup used here has a finite pulse duration that is variable between 0.5 and 1.0 μ s. In principle, supersonic turbulent flow structures can be blurred by such a finite pulse duration, but this blur was found to be insignificant for the case of the boundary layer investigated here. The finite pulse rise and fall times also affect the determination of the time interval between the images in a “PIV” pair. For present purposes the interframe time interval was taken to be the interval between the initiation of each pulse, and was termed “pulse separation”.

The small physical size of LEDs allows them to be combined in dense arrays to increase the overall illumination. The 2x2 array used here is sufficient for recording schlieren images only when the image is focused directly into the camera lens instead of onto a ground-glass image plane. This causes a depth-of-focus penalty as described earlier. We have found that that the use of a ground-glass screen in the image plane decreases the PIV image illumination by 2-4 stops due to light scattering. Even with a holographic screen in the image plane, the illumination was still insufficient. However, referring to Figure 3, 2 additional stops of source illumination could readily be had by using a 4x4 rather than a 2x2 LED array. Future work will address this issue by way of a larger LED array, subject to the requirement that the incident light beam must be accommodated by the main imaging lens aperture, A , in Figure 1.

II.C. Supersonic Wind Tunnel Facility

These experiments were performed in the Penn State Gas Dynamics Laboratory’s supersonic wind tunnel facility. This is an intermittent blowdown facility with a test section size of 15 x 17 x 60 cm. A 57 m³, 2 MPa pressure reservoir provides a test duration of more than 30 seconds every 20 minutes. The facility has a continuously-variable Mach number capability over the range of Mach 1.5 to 4.0 by way of an asymmetric sliding-block nozzle.

All measurements reported here were made at a freestream Mach number of 3 with a nominal stagnation pressure and temperature of $6.9 \cdot 10^5$ Pa and 287K, respectively. The boundary layer measured here was on the wind tunnel test section floor, as shown schematically in Figure 5. This boundary layer develops in a pressure gradient on the curved lower wall of the long asymmetric nozzle, thus it is not expected to be identical to a flat-plate boundary layer.

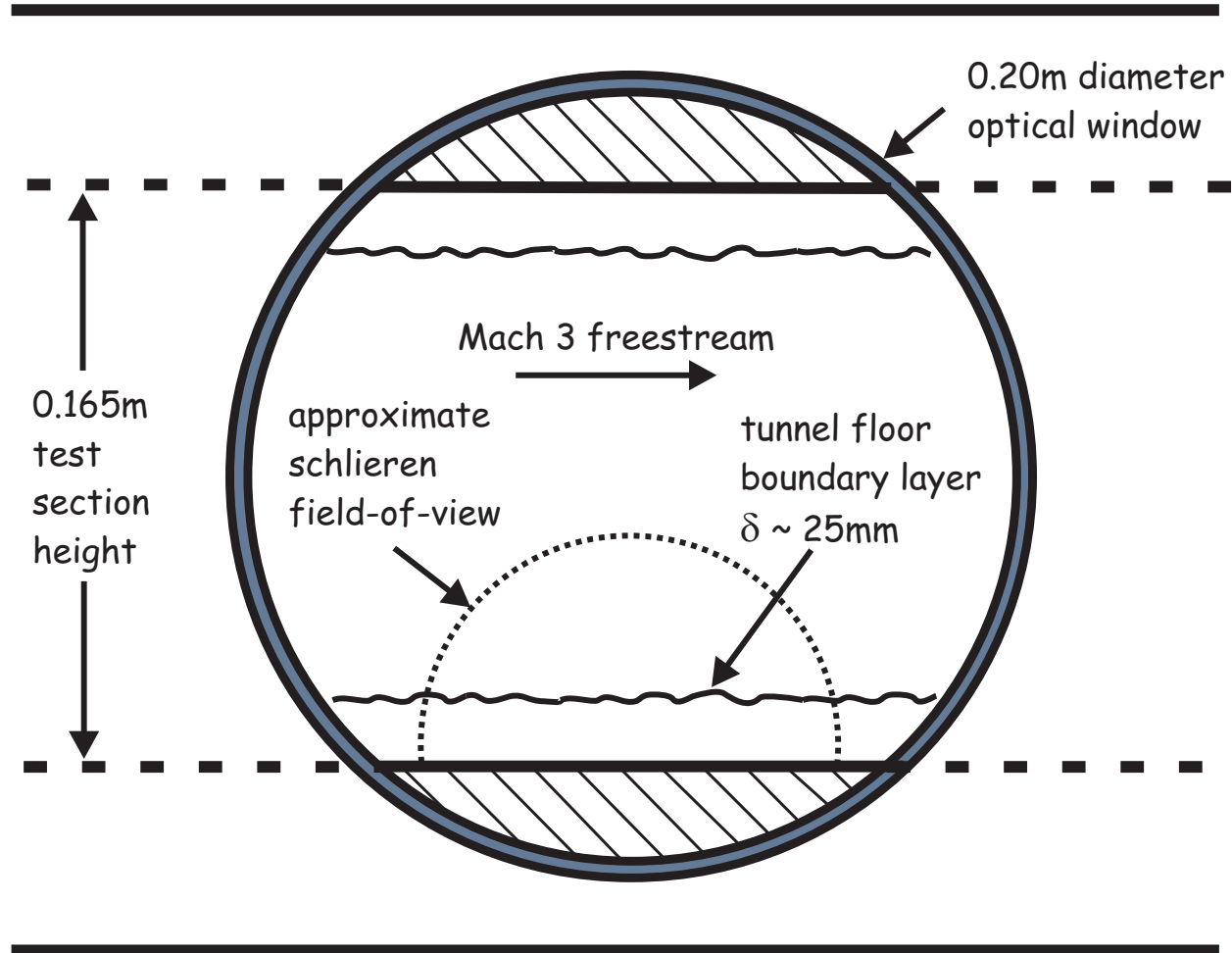


Figure 5. A schematic showing the supersonic test section and the approximate area being imaged

A boundary-layer pitot-pressure survey performed at Mach 2.8 by Garg and Settles¹¹ was used as the benchmark for current schlieren velocimetry measurements. (Only a negligible boundary-layer structure change is expected between Mach 2.8 and 3.¹³) The wind-tunnel walls were approximately adiabatic, and the freestream turbulence level was approximately 1-2%. Boundary-layer parameters, as previously determined from pitot-pressure surveys assuming constant total temperature across the boundary-layer,¹¹ were: $\delta = 25\text{mm}$, $\delta^* = 1.7\text{mm}$, $Re_\theta = 9000$, and $c_f = 0.0010$.

Limited schlieren “PIV” boundary-layer measurements were also performed at freestream Mach numbers of 2 and 2.5. These showed that, as expected, the schlieren results are strongly dependent on the freestream density level. At Mach 2 the freestream density is twice as large as at Mach 3, and the focusing schlieren images showed better definition of the turbulent structures. However, only the results obtained at Mach 3

are considered here.

II.D. PIV System and Image Processing

A PCO 1600 camera was used to record the focusing-schlieren image pairs. This camera provides 1600x1200 pixel resolution with 14bit pixel depth, and captures image pairs at about 15Hz, with an average of 150 image pairs per experiment. The large pixel range and field of view were found to improve the ability to image weak schlieren disturbances. The camera exposure for the first image of a pair, “frame A”, was deliberately set to be slightly longer than the first LED pulse duration. The exposure of the second image, “frame B”, was determined by the camera readout time and was typically several milliseconds. Frame A was therefore always precisely exposed, but frame B sometimes suffered areas of overexposure due to ambient light, even though the experiments were performed in a darkened laboratory.

Compressible boundary layer structures are readily visible in the schlieren images recorded here, but are still typically image-processed to improve their contrast. For each image sequence, a background image is created by averaging all images within the data set obtained during a wind-tunnel run. Different background images are determined for frames A and B. Then the common background image is subtracted from each PIV image, which is subsequently readjusted to normalized pixel values ranging between 0 (black) and 1 (white). Finally, each image is blurred with a 3x3-pixel averaging filter to remove fine-scale noise before processing for velocimetry. A sample image pair, showing both the raw and processed PIV images, is given in Figure 6. The flow is from left to right in these images, as clearly identified by the inclination of the turbulent structures.

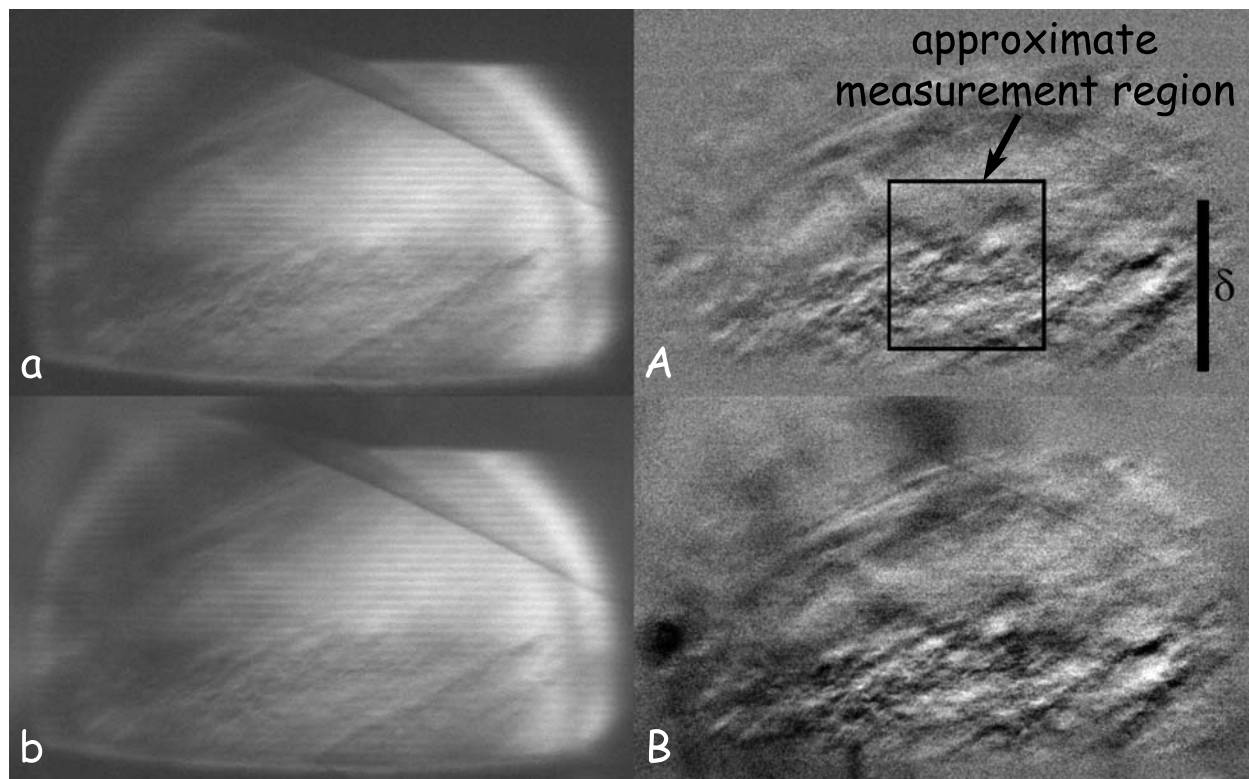


Figure 6. Sample focusing schlieren images showing the turbulent boundary layer structures. The original images (a) and (b) are image processed to produce the final images (A) and (B), respectively. The final images show intermittency along the boundary layer edge, which is labeled in (A) along with the approximate measurement region. Also visible in the images is a conical probe in the freestream and its associated compressible phenomena; the probe is present for alignment purposes only and does not affect the present measurements.

One drawback of using a simple lens to project the schlieren image into the camera lens is that some image distortion can occur. This image distortion can be seen in Figure 6a: the flat wind tunnel floor is clearly distorted into an arc. This image distortion can be accounted for within the PIV calibration procedure or limited by using a smaller measurement region where the distortion is not significant. The measurement region as outlined in Figure 6 is calibrated and positioned to limit the influence of image distortion. The

measurement region extends from about $0.1 < \frac{y}{\delta} < 1.0$, as measured from a calibration image. The large PIV interrogation window required here prevented measurements of the velocity profile at heights of $\frac{y}{\delta} < 0.1$.

Commercial PIV software from Idtpiv.com was used to analyze the image pairs. The correlations were performed using the adaptive interrogation mode available in this software, and an interrogation window of about 40 pixels. This interrogation window size was determined by the average size of the turbulent structures to be correlated. It was found that the interrogation window should be larger than the average turbulent structure size for best results. A streamwise image offset of 2 pixels was also used to compensate for the long interframe time interval, thus improving the correlation.

II.E. Conventional Shadowgraph Visualization

A parallel-light “focused” shadowgraph system⁷ was also used here to image the boundary layer. This shadowgraph system featured two 152mm diameter, $f/5.67$ lenses, and it imaged the same approximate region of the boundary layer described earlier. Illumination was provided by a single 5mm white LED, pulsed in the same manner as described above. The PIV camera was focused at about a 20cm offset from the wind tunnel centerline in order to provide sufficient shadowgraph sensitivity.

The purpose of shadowgraphy was to compare the focusing-schlieren results to results obtained from a conventional parallel-light system that integrates refractive effects across the entire wind-tunnel test section, including sidewall boundary layers. (Note that Jonassen et al.² have shown that the schlieren and shadowgraph techniques produce very similar results when used for seedless “PIV” of turbulent refractive flows.) The wind tunnel test section width is approximately 6 times the height of the tunnel-floor boundary layer, thus the flow can be regarded as two-dimensional in the mean and a useful comparison between focusing and integrating optics can be made. Figure 7 shows a conventional shadowgraph boundary-layer image compared to one of the present focusing-schlieren images; both images have been image processed.

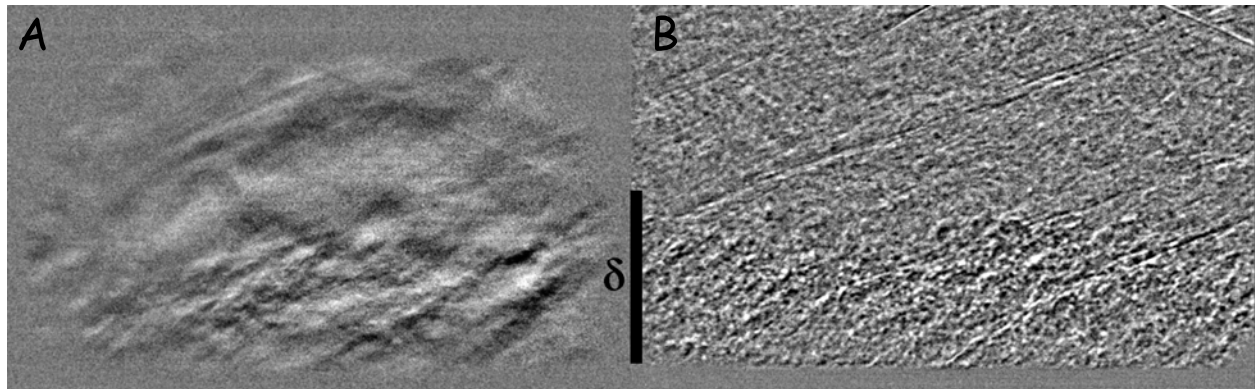


Figure 7. A focusing schlieren image (A) is compared to a conventional shadowgraph image (B) to show the focusing effect and its influence on determining the edge of the boundary layer, as labeled.

The conventional shadowgraph image reveals finer-scale turbulence than the focusing schlieren image, which improves correlations with the PIV software. The image also shows turbulent structures throughout the field of view, even outside the tunnel-floor boundary layer, as a result of the sidewall boundary layers on the glass windows. There is thus no clear edge to the boundary layer in the shadowgrams, although some larger structures near the edge can be distinguished if one has a priori knowledge of their existence.

III. Experimental Results and Discussion

III.A. Turbulent Boundary Layer Intermittency

An important factor in schlieren “PIV” velocimetry is turbulent intermittency. Intermittency implies that turbulent structures and low-turbulence-“laminar” flow from the freestream coexist heterogeneously within the outer part of the boundary layer. The mass-averaged velocity in an intermittent region can be inferred from pitot-pressure surveys, but the low-turbulence regions are problematic for schlieren “PIV” because the lack of turbulent structures is analogous to a lack of PIV “particles”. Thus, in the intermittent regions of a flow, schlieren “PIV” suffers from a problem similar to inadequate seeding in traditional PIV. Understanding

the intermittency in the measurement region is therefore essential to the interpretation of schlieren “PIV” results.

The intermittency function, γ , for an incompressible turbulent boundary layer was defined by Klebanoff¹⁴ as a function of height within the boundary layer, $\frac{y}{\delta}$:

$$\gamma = \frac{1}{2} (1 - \operatorname{erf} \zeta) \quad (3)$$

where

$$\zeta = \left(\sqrt{2} \frac{\sigma}{\delta} \right)^{-1} \left(\frac{y}{\delta} - 0.78 \right) \quad (4)$$

and the standard deviation, σ , is defined as:

$$\sigma = 0.14\delta \quad (5)$$

Thus defined, the intermittency function varies from 1, indicating that turbulent structures are always present, to 0 where structures do not exist, as is plotted in Figure 8. From this approximation, an effective “edge” to the turbulent boundary layer can be approximated at a mean height of $\frac{y}{\delta} \approx 0.78$. This height represents the location where structures are present approximately 50% of the time and can be observed in Figure 7. The approximation also shows that the instantaneous boundary layer edge essentially never extends outside the region $0.4 < \frac{y}{\delta} < 1.2$. The ability to perform accurate schlieren “PIV” measurements is restricted to regions of the flow where at least some turbulent structures are present, therefore it is expected that schlieren PIV results will deteriorate in the turbulent boundary layer (compared to the pitot-survey benchmark) when $\frac{y}{\delta} > 0.4$. Although this approximation is for an incompressible turbulent boundary layer, the turbulent structure of the Mach 3 boundary layer is fully expected to be similar to the incompressible case, as first suggested by Morkovin many years ago.¹³

III.B. Focusing-Schlieren PIV Results

Figure 8 presents the results obtained for the boundary-layer convective-velocity profile as determined from focusing-schlieren PIV alongside the benchmark pitot-pressure survey result obtained by Garg and Settles.¹¹ It is clear from this figure that the correct convection velocity cannot be measured using a typical PIV ensemble average. This is because turbulent structures are not always present due to intermittency, causing the ensemble average to be low. Further reduction in the ensemble average is likely due to limitations on the visibility and size of the turbulent structures.

The focusing-schlieren images of the turbulent structures were typically of low contrast and lacking sufficient fine-scale turbulence to allow the PIV algorithm to correlate properly. Instead the algorithm sometimes correlated on nondescript regions, resulting in non-physical, artificially-low velocities that were nonetheless included in a standard ensemble average. If these low velocities are removed, by considering only the top 2% of measured velocities, then the resulting velocity profile approaches the established pitot-survey benchmark for $\frac{y}{\delta} < 0.6$. However, this technique of isolating only the largest velocities requires a priori knowledge of the flowfield and is imprecise due to the ambiguity in which structures the PIV software is actually correlating upon. But also note that it is unphysical to expect eddy velocities higher than the local convective velocity to be measured, thus considering only the fastest data has some justification.

For $\frac{y}{\delta} > 0.6$ the focusing-schlieren PIV results deteriorate quickly, even when only the maximum velocity correlations are accepted. The turbulent structures in this region are sparse, of low-contrast, and significantly larger than is appropriate for analysis with the present PIV algorithm. The structures in this region can, however, be tracked through “manual PIV” as was done by Papamoschou,^{4,5} whereupon the results approach the expected pitot-survey benchmark significant human-estimation error.

III.C. Focusing Schlieren versus Conventional Shadowgraphy

Conventional parallel-light shadowgraphy, described earlier, provides two advantages over focusing schlieren for “PIV” analysis: the resolution of smaller-scale structures and improved contrast. As presented in Figure 7, the shadowgraph beam integrates across the entire test section and reveals many small-scale, high-contrast turbulent structures dispersed throughout the boundary layer. These structures are better for analysis using a commercial PIV algorithm. As presented in Figure 9, the results of shadowgraph “PIV” are somewhat

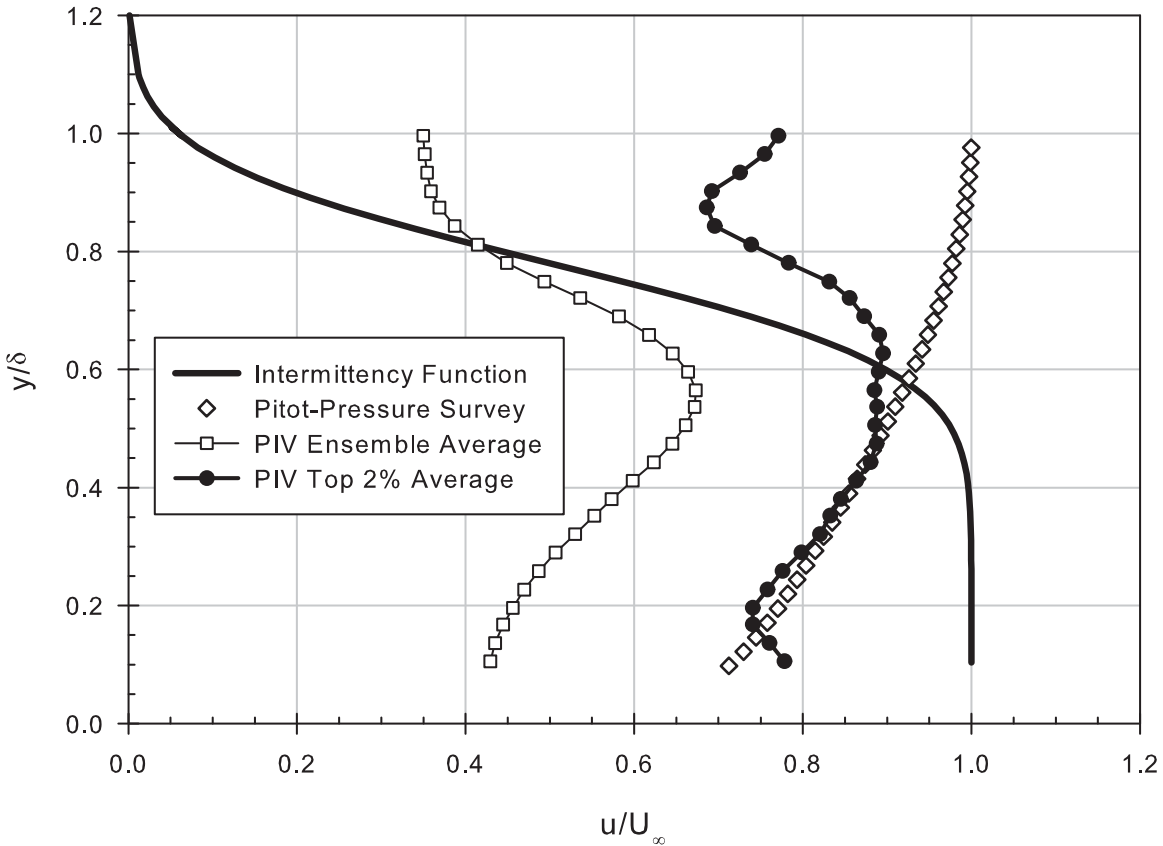


Figure 8. Velocity profile data measured with pitot-pressure survey and focusing-schlieren PIV, also showing turbulent boundary layer intermittency function

better than those presented above for focusing-schlieren “PIV”. For the present application, with a wind tunnel test section width to boundary-layer height ratio of approximately 6, the flowfield is approximately two-dimensional, thus optical integration including the sidewall boundary layers has little influence on the results.

The ensemble-average data again show a systematic deviation from the expected profile, due to artificially-low velocities being averaged when no structures are present within an interrogation window. Isolation of the top 10% of the calculated velocities results in good agreement with the pitot-survey benchmark. The ability to utilize a larger percentage of the calculated velocity correlations is directly related to the increase in structure frequency and visibility in the shadowgraph case.

These shadowgraph results also show a better ability to perform measurements within the intermittent region of the boundary layer. The present data show the local convective velocity to be slightly less than the mean velocity derived from a pitot-survey, which agrees with previous work by Spina et al.,¹⁵ who measured large-scale-structure motion using hot-wire anemometry. This result, however, disagrees with the previous work of Garg and Settles.¹¹ These findings highlight an incomplete understanding of the local turbulent convective speed in the intermittent region of supersonic boundary layers. Future improvements to the reliability and accuracy of the PIV correlation algorithm for this application, combined with both focusing-schlieren and non-focusing shadowgraph “PIV”, are expected to improve our physical understanding of this intermittent eddy motion.

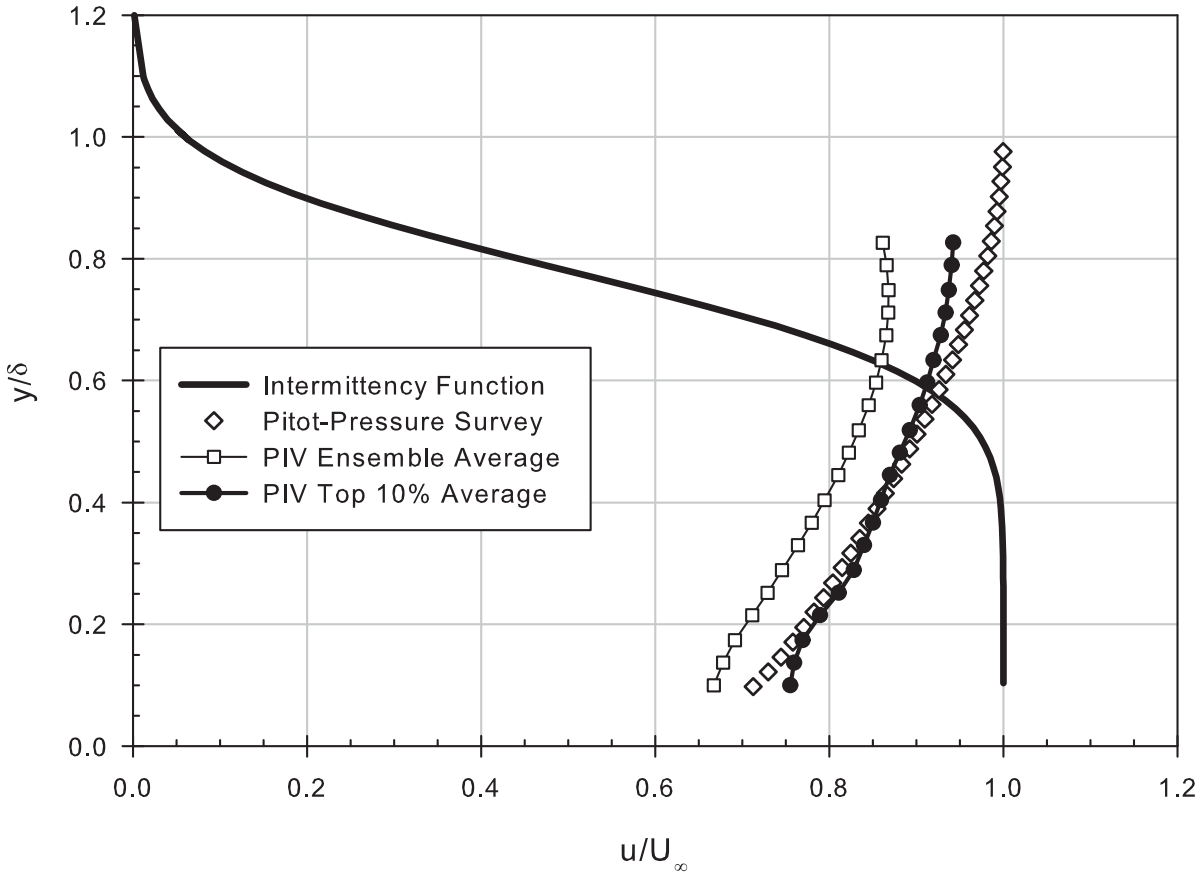


Figure 9. Velocity profile data measured with pitot-pressure survey and shadowgraph PIV, also showing turbulent boundary layer intermittency function

IV. Conclusions

A focusing-schlieren optical system has been developed for performing velocity measurements of refractive-turbulent flows using commercial particle image velocimetry algorithms. Focusing-schlieren “PIV” is a potentially-important seedless-velocimetry technique that is capable of performing near-planar velocimetry measurements, using naturally-occurring turbulent eddies within a flow as PIV “particles”.

The velocity measurements from the focusing-schlieren “PIV” were compared to similar but parallel-light shadowgraph “PIV” results and a previous pitot-pressure survey profile of a compressible turbulent boundary layer on the floor of the Penn State Gas Dynamics Laboratory’s supersonic wind tunnel. Reasonable agreement was demonstrated with the pitot-survey benchmark. The ability to perform accurate schlieren and shadowgraph “PIV” measurements in this turbulent flow, however, is limited by the inherent intermittency of the turbulent boundary layer. Because these PIV techniques rely on turbulent structures as “particles”, the presence of intermittent low-turbulence regions within the boundary layer currently precludes the ability to perform accurate “turnkey” PIV measurements of the mean convective velocity.

Focusing schlieren, with a limited depth-of-focus and limited contrast, does not perform well with the present commercial PIV software. As the depth-of-focus decreases, schlieren sensitivity, image contrast, and the frequency of turbulent eddies also decrease while the eddy feature size increases. All the factors hinder the ability to accurately process large sequences of schlieren images with standard PIV settings and analysis. For the present system, with a depth-of-focus of approximately $\pm 40\text{mm}$, images can be obtained that contain sufficient contrast and eddy density to perform an accurate PIV analysis. The ensemble-averaged data, however, consistently includes low-velocity correlations in areas where no eddies exist. Physical arguments,

based on a priori knowledge of the flowfield, result in the isolation of the top percentile of the data to compare with the benchmark. This technique works for this application to turbulent boundary layers, but limits the utility of focusing-schlieren “PIV” as a “turnkey” approach to seedless velocimetry.

Shadowgraphy results in higher-contrast and feature-dense images that are more suitable for PIV analysis. The shadowgraph integration along the optical path produces path-averaged velocity measurements, but can still be appropriate for nearly-two-dimensional flowfields such as the present compressible boundary layer. Increased feature density results in improved correlations throughout the boundary layer, including the intermittent regions. Isolation of the highest-percentile velocity measurements is still required for accuracy, but results can be extended further outward toward the freestream. The shadowgraph results through the intermittent region have shown that the turbulent structures may not be moving at the local mean-boundary-layer velocity.

Although intermittency has limited the current results, its influence remains primarily confined to a data-processing issue. An improved PIV algorithm, with considerations for schlieren images containing intermittent and low-contrast regions, would be a big improvement. With present commercial PIV codes, processing schlieren PIV images requires an a priori knowledge of the flowfield and the intermittency distribution.

LEDs were used as the light sources for both present imaging systems. They show significant advantages over conventional laser illumination for PIV. The LED light array developed here produced high-output non-coherent light that allowed resulting schlieren and shadow images to be post-processed, whereas this post-processing was difficult or impossible with the previous coherent laser illumination. The LEDs are also compact, allowing the creation of LED arrays for use in a range of visualization systems. The use of a finite LED light pulse was also shown to not limit the ability to perform the present measurements, although the pulse length should be independently evaluated for a given flowfield application.

Acknowledgments

This work was funded by subcontract SB08-004 FA8650-08-C-3828 from Spectral Energies LLC, based on an SBIR contract from the Air Force Research Laboratory, Wright-Patterson Air Force Base. The authors would like to thank the following for their support throughout this work: Captain C. McGaha, J.D. Miller, L.J. Dodson-Dreibelbis, and R.A. Kreuter, who designed and built the LED illuminator.

References

- ¹Raffel, M., Willert, C. E., and Kompenhans, J., *Particle image velocimetry*, Springer, 3rd ed., 1998.
- ²Jonassen, D. R., Settles, G. S., and Tronosky, M. D., “Schlieren “PIV” for turbulent flows,” *Optics and Lasers in Engineering*, Vol. 44, No. 3-4, 2006, pp. 190 – 207.
- ³Townend, H., “A method of airflow cinematography capable of quantitative analysis,” *Journal of the Aeronautical Sciences*, Vol. 3, 1936, pp. 343–352.
- ⁴Papamoschou, D., “A 2-spark schlieren system for very-high velocity-measurement,” *Experiments In Fluids*, Vol. 7, No. 5, 1989, pp. 354–356.
- ⁵Papamoschou, D., “Structure of the compressible turbulent shear-layer,” *AIAA Journal*, Vol. 29, No. 5, 1991, pp. 680–681.
- ⁶Fu, S. and Wu, Y., “Detection of velocity distribution of a flow field using sequences of Schlieren images,” *Optical Engineering*, Vol. 40, No. 8, 2001, pp. 1661 – 1666.
- ⁷Settles, G. S., *Schlieren and shadowgraph techniques: Visualizing phenomena in transparent media*, Springer-Verlag, 2001.
- ⁸Schardin, H., “Die schlierenverfahren und ihre anwendungen,” *Ergebnisse der Exakten Naturwissenschaften*, Vol. 20, 1942, pp. 303–439.
- ⁹Weinstein, L., “Large-field high-brightness focusing schlieren system,” *AIAA J.*, Vol. 31, 1993, pp. 1250–1225.
- ¹⁰Alvi, F. S., Settles, G. S., and Weinstein, L. M., “A sharp-focusing schlieren optical deflectometer,” *Proc. AIAA Aerospace Sciences Meeting and Exhibit, Reno, NV, Jan. 11-14, 1993*, Vol. Paper 93-0629, AIAA, 1993.
- ¹¹Garg, S. and Settles, G. S., “Measurements of a supersonic turbulent boundary layer by focusing schlieren deflectometry,” *Experiments In Fluids*, Vol. 25, No. 3, 1998, pp. 254–264.
- ¹²O’Hagan, W., McKenna, M., Sherrington, D., Rolinski, O., and Birch, D., “MHz LED source for nanosecond fluorescence sensing,” *Measurement Science & Technology*, Vol. 13, 2002, pp. 84–91.
- ¹³Spina, E., Smits, A., and Robinson, S., “The physics of supersonic turbulent boundary-layers,” *Annual Review of Fluid Mechanics*, Vol. 26, 1994, pp. 287–319.
- ¹⁴Klebanoff, P. S., “Characteristics of turbulence in a boundary layer with zero pressure gradient,” Tech. Rep. 1247, National Advisory Committee for Aeronautics, 1955.

¹⁵Spina, E., Donovan, J., and Smits, A., "Convection Velocity in Supersonic Turbulent Boundary-Layers," *Physics of Fluids A-Fluid Dynamics*, Vol. 3, No. 12, 1991, pp. 3124–3126.